A Modelica Implementation of an Organic Rankine Cycle

Hongxiang Fu[1] Ettore Zanetti[1] Jianjun Hu[1] David Blum[1] Michael Wetter[1]

[1]Building Technology and Urban Systems Division, Lawrence Berkeley National Laboratory, USA,
{hcasperfu,ezanetti,jianjunhu,dhblum,mwetter}@lbl.gov

Abstract

Organic Rankine cycle (ORC) systems generate power from low-grade heat sources, such as geothermal sources and industrial waste heat. A key feature is that a working fluid is selected to match the temperature of the source. With the vast pool of candidate working fluids comes the challenge of developing a large number of robust thermodynamic media models. We implemented a subcritical ORC model in Modelica that uses working fluid data records and interpolation schemes in lieu of thermodynamic medium evaluation for energy recovery estimation. This is a component model that can be integrated into a larger energy system model. It does not require detailed thermodynamic, heat transfer, or machine analysis. Our ORC model fills a gap where working fluids are ready to choose or easy to add, and at the same time can be integrated into an energy system.

Keywords: organic Rankine cycle, media model, component model

1 Introduction

Organic Rankine cycle (ORC) systems have been an important waste heat recovery technology used to generate power from low-grade heat sources, such as geothermal sources and industrial process waste heat. It is particularly valuable to building and district energy applications, because in these areas both the electric power generated by the expander and heat rejected from the condenser can be used. Under the current background of decarbonisation (U.S. DOE 2024), it is valuable to model such systems for utilisation of renewable energy in district energy systems design.

ORC systems typically use a working fluid whose boiling point is matched to a specific waste heat source (U.S. DOE 2021). This versatility also poses a significant challenge: Developing robust and computationally efficient medium models for a wide range of candidate working fluids is a time-consuming and complex task. To accommodate a wide range of heat sources, including geothermal sources at 80°C to biomass sources at 500°C, there can be hundreds of potentially suitable substances (Bao and Zhao 2013). Studies on working fluid selection routinely examined tens of candidates. For example Saleh et al. (2007) investigated 31 pure fluids, and the number goes up substantially if mixtures were considered due to the possibility of combinations and mixing ratios (Abadi and Kim 2017).

There are existing open-source Modelica libraries that support modelling of thermodynamic cycles. The DLR ThermofluidStream library (Zimmer 2020; Zimmer, Meißner, and Weber 2022) has five refrigerant models that can be used for ORC (as of Version 1.1.0). It provides a helpful medium model template, but defers the implementation of additional robust models to the user, which remains challenging for non-experts. The ThermoPower library (Casella and Leva 2005) provides component models as well as control blocks suitable for thermodynamic cycle and system modelling. However, it is not specifically geared towards ORC modelling and additional component and medium models are needed. The ThermoCycle library (Quoilin, Desideri, et al. 2014; Oliveira, Iten, and Matos 2022) has Rankine and Brayton cycle models with detailed components such as heat exchangers and turbines, as well as control blocks. However, it only supports the steam cycle and not the ORC. It also requires external dependency for the medium models through the Modelica ExternalMedia library (Modelica 3rd-party libraries 2023) to the open-source software CoolProp (Bell et al. 2014) and the commercial software FluidProp (Asimptote 2023).

Multi-phase fluid property computations needed for ORC models are numerically challenging because of sharp derivative changes at phase transition. Naïve integration with detailed medium models can lead to long computation times and convergence problems. Literature has reported that, using professional software such as the Modelica ExternalMedia library for medium property computations was not enough. Interpolation methods at the phase transitions led to one order of magnitude shorter simulation time (Quoilin, Van Den Broek, et al. 2013; Twomey 2016).

Because of these challenges, it is understandable that we have not found an open-source ORC model with a collection of medium models that do not require use of an external code for media calculations. This is a drawback because selecting a working fluid with properties matching the waste heat source is a key step in the ORC system design. The following gap exists in the literature: Studies with a large pool of working fluids are usually limited at thermodynamic analysis; in the meantime, studies that performed detailed machine analysis or control designs often either only used one specific working fluid or resorted to external code for medium models. We there-

fore report a Modelica implementation of the ORC model with energy system integration that comes with ready-to-use and easy-to-add working fluid models to fill this gap. Our method is based on data records of working fluids converted from CoolProp and are used together with interpolation schemes in lieu of detailed thermodynamic fluid property computation. It improves upon existing open-source models we found in the literature as follows: First, all code is contained in one standalone Modelica library. Because there is no need to link to external code, usability and compatibility are improved. Second, unlike developing full-fledged media models, adding more media records to the package is easy for users, which suits the nature of ORC system design, allowing consideration of a broad pool of candidate working fluids. We have currently implemented ten fluids as listed in Table 2. We selected CoolProp as the source of fluid properties because it is open-source and offers wrappers for various languages and environments. It is important to note that any software that provides thermodynamic fluid properties can be used to generate the data records. Furthermore, because the property data are stored in Modelica records once generated, the choice of fluid property sources becomes irrelevant.

The vast pool of ORC working fluids manifests the versatility and also challenges of ORC modelling. Our method circumvents this challenge by using specialised and interpolation-based medium models that forego computationally challenging thermodynamic property evaluations. The result is a fast and robust model to obtain energy recovery estimation for an ORC component that can be integrated into an energy system for system-level design and analysis.

2 System Description

We consider a subcritical organic Rankine cycle as a bottoming cycle to recover energy from a hot fluid stream. Figure 1 is its concept schematic.

The system is not controlled to track any load, electric or thermal, and all generated power is assumed to be consumed and heat dissipated. The working fluid evaporating temperature $T_{w,eva}$ is a user-specified parameter. This is in line with the optimisation results reported by Quoilin, Aumann, et al. (2011) and Imran et al. (2020) that keeping a constant $T_{w,eva}$ was a common and proper control strategy for small-scale ORCs.

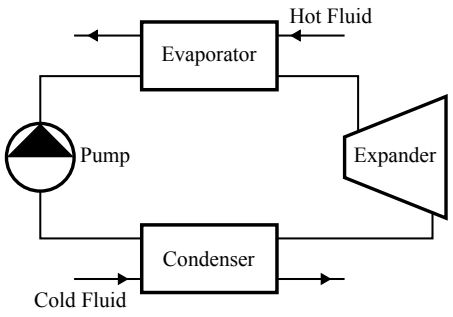

Figure 1. Schematic of the modelled ORC system.

The heat source is variable in terms of temperature and flow rate and an ORC system needs to accommodate to that. To achieve this, the working fluid flow rate $\dot{m}_w$ is controlled to maintain the evaporator pinch point temperature difference $\Delta T_{pin,eva}$. The following constraints are in place:

- The mass flow rate $\dot{m}_w$ will not go higher than a set upper limit. Rather, $\dot{m}_w$ stays at the user-specified upper limit and $\Delta T_{pin,eva}$ increases beyond its set point. This may happen when the incoming hot fluid has a high flow rate or a high incoming temperature, i.e., it carries more energy than the cycle is sized to process.
- When $\dot{m}_w$ needs to go lower than a set lower limit, $\dot{m}_w$ is set to zero and the cycle is switched off. This may happen when the incoming waste heat fluid has a low flow rate or a low incoming temperature, i.e., it carries too little energy.

On the condenser side, an upper limit is needed for the working fluid condensing temperature $T_{w,con}$ to maintain sufficient pressure difference between evaporator and condenser. In some applications, a lower limit is also needed so that the condensing pressure p_{con} remains above the atmospheric pressure to prevent a vacuum. However, unlike the evaporator control which actuates on the working fluid pump, the condenser is controlled via the cold fluid (Manente et al. 2013; Nami et al. 2018). Implementation of these constraints are therefore the responsibility of the encompassing system rather than the component.

3 Model Description

This section describes the model implemented in Modelica.

3.1 Assumptions

The model uses the idealised thermodynamic cycle shown in Figure 2. Depending on the type of the fluid, the cycle has two variants. Figure 2(a) shows a *dry fluid* whose saturated vapour line has a section with positive slope. This implies that no superheating is needed. Figure 2(b) shows a *wet fluid* where superheating is required to avoid liquid formation in the turbine which would cause damage. In this case we assume that the superheating is controlled to be minimised, i.e. the expander outlet state is exactly on the saturation line. How this affects the calculation will be explained in section 3.3.2. There is no subcooling out of the condenser outlet. For any given working fluid, wet or dry, the cycle is fully determined by the working fluid evaporating temperature $T_{w,eva}$, working fluid condensing temperature $T_{w,con}$, the expander efficiency η_{exp}, and the pump efficiency η_{pum}. We will further explain how the working fluid property influences the computation in section 3.3.2.

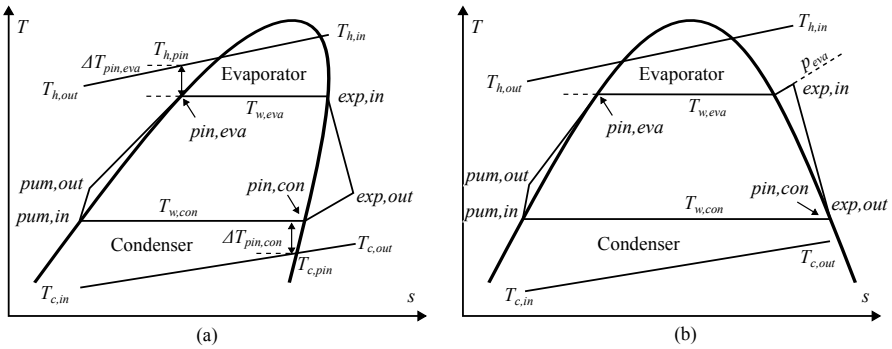

Figure 2. Idealised thermodynamic cycle used to implement the ORC. (a) For a dry fluid, the cycle has no superheating and the expansion starts on the saturation line; (b) For a wet fluid, the cycle is superheated and the expansion ends on the saturation line.

The evaporator pinch point (PP) is at the *bubble point* (where evaporation starts) and the condenser PP is at the *dew point* (where condensation starts). Pan and Shi (2016) discussed where the PP can occur at other places in a phase-change heat exchanger, but our model assumes the PP's are only at these two places.

The evaporation and condensation processes are assumed isobaric. This model therefore excludes any working fluid with a temperature glide, such as zeotropic mixtures. It also means there is no pressure loss along the pipes.

The thermodynamic cycle of the working fluid is steady-state, but the hot and cold fluid streams can be configured to be either steady-state or dynamic. The model does not perform detailed machine analysis. The mass flow rate $\dot{m}_w$ in the model is solved analytically to meet the set point, subject to the described constraints, instead of being controlled using feedback control. For the condenser, at the component level, we use the `assert()` function with `AssertionLevel.error` to stop the simulation when $T_{w,eva} - T_{w,con} < 1$ K and we use `assert()` with `AssertionLevel.warning` when $p_{con} < 101325$ Pa.

3.2 Governing Equations

The evaporator heat exchange is

$$\dot{Q}_{eva} = \dot{m}_h \, c_{p,h} \, (T_{h,out} - T_{h,in}), \tag{1}$$

$$\dot{Q}_{eva} = \dot{m}_w \, (h_{pum,out} - h_{exp,in}), \tag{2}$$

with evaporation taking place at a constant, user-specified temperature $T_{w,eva}$. The evaporator PP difference $\Delta T_{pin,eva}$ is also specified by the user, which is used in

$$\frac{T_{h,pin} - T_{h,out}}{T_{h,in} - T_{h,out}} = \frac{h_{eva,pin} - h_{pum,out}}{h_{exp,in} - h_{pum,out}}, \tag{3}$$

$$\Delta T_{pin,eva} = T_{h,pin} - T_{w,eva}. \tag{4}$$

The condenser side uses the same equations with the variables replaced by their condenser counterparts where appropriate:

$$\dot{Q}_{con} = \dot{m}_c \, c_{p,c} \, (T_{c,out} - T_{c,in}), \tag{5}$$

$$\dot{Q}_{con} = \dot{m}_w \, (h_{exp,out} - h_{pum,in}), \tag{6}$$

$$\frac{T_{c,pin} - T_{c,in}}{T_{c,out} - T_{c,in}} = \frac{h_{con,pin} - h_{pum,in}}{h_{exp,out} - h_{pum,in}}, \tag{7}$$

$$\Delta T_{pin,con} = T_{w,con} - T_{c,pin}. \tag{8}$$

Equations 1 through 8 are eight equations and eight unknowns: $\dot{Q}_{eva}$, $T_{h,out}$, $\dot{m}_w$, $T_{pin,eva}$, $\dot{Q}_{con}$, $T_{c,out}$, $T_{pin,con}$, and $T_{w,con}$. Note that all enthalpy values are known through $T_{w,eva}$, $T_{w,con}$, η_{exp}, and η_{pum}. This will be explained in detailed in section 3.3.

The expander power P_{exp}, pump power P_{pum}, electrical power generated P_{ele}, and cycle thermal efficiency η_{the} are

$$P_{exp} = \dot{m}_w \, (h_{exp,out} - h_{exp,in}), \tag{9}$$

$$P_{pum} = \dot{m}_w \, (h_{pum,out} - h_{pum,in}), \tag{10}$$

$$P_{ele} = P_{exp} + P_{pum} \tag{11}$$

$$\eta_{the} = \frac{-P_{ele}}{\dot{Q}_{eva}}. \tag{12}$$

Note that all energy transfer and power terms follow the sign convention where energy into the cycle is positive. Therefore, $\dot{Q}_{eva}$ and P_{pum} are positive; $\dot{Q}_{con}$ and P_{ele} are negative.

The information flow of the model is summarised in Table 1.

3.3 Thermodynamic Properties

The thermodynamic properties of the working fluid are not computed by a medium model as in `Modelica.Media`, but rather by interpolation schemes. Support points for interpolation are given on the saturated liquid line, saturated vapor line, and a superheated vapor line (called the *reference line*), as shown in Figure 3. Each support curve consists of an array of specific enthalpy, specific entropy, temperature, and pressure. The temperature and pressure arrays are paired as the corresponding saturation values of each other. By default we set the reference line to be 30 K higher than the saturated vapor line. We determined the

User-specified parameters		Inputs		Outputs	
$T_{w,eva}$	Working fluid evaporating temperature,	$T_{h,in}$	Evaporator hot fluid incoming temperature,	$\dot{m}_w$	Working fluid flow rate,
$\Delta T_{pin,eva}$	Evaporator PP temperature difference,	$\dot{m}_h$	Evaporator hot fluid flow rate,	$T_{w,con}$	Working fluid condensing temperature,
$\Delta T_{pin,con}$	Condenser PP temperature difference.	$T_{c,in}$	Condenser cold fluid incoming temperature,	$T_{h,out}$	Evaporator hot fluid outgoing temperature,
η_{exp}	Expander efficiency	$\dot{m}_c$	Condenser cold fluid flow rate	$T_{c,out}$	Condenser cold fluid outgoing temperature,
η_{pum}	Pump efficiency			$\dot{Q}_{eva}$	Evaporator heat flow rate,
				$\dot{Q}_{con}$	Condenser heat flow rate,
				P_{exp}	Expander power output,
				P_{pum}	Pump power consumption.

Table 1. Information flow of the model

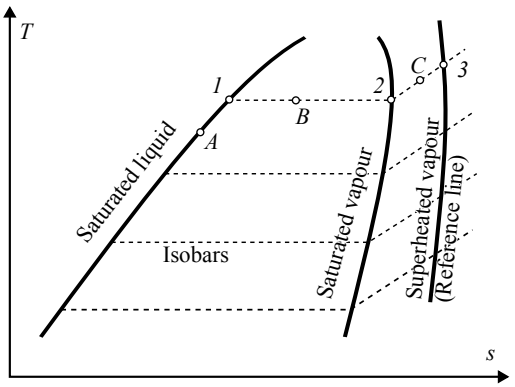

Figure 3. Support curves for interpolation. A, B, and C are example points on a saturation line, between the two saturation lines, and in the superheated region, respective. 1, 2, and 3 are example reference points on the saturation lines and the reference line used to find the example points.

values of these support points using CoolProp (Bell et al. 2014) with its Python wrapper. It should be noted that any software that provides thermodynamic fluid properties can be used to find these points.

3.3.1 Interpolation Schemes

We will demonstrate the interpolation schemes using Figure 3.

- On the saturation line, the specific enthalpy, specific entropy or density, here labeled as y_A, are obtained using cubic Hermite spline interpolation as

$$y_A = s(u_A, d) \tag{13}$$

  where $s(\cdot,\cdot)$ is a cubic Hermite spline, u_A is the input property, and d are the support points. For the saturation curves, the user can configure the model to use either the saturation pressure or the saturation temperature for u_A; for the reference line in Figure 3, u_A is the pressure.

- If the fluid is wet, the isentropic expander outlet point would be in between the saturation lines, shown in Figure 4(b). In this case, its enthalpy h_B is obtained from

$$\frac{h_B - h_1}{s_B - s_1} = \frac{h_2 - h_1}{s_2 - s_1} \tag{14}$$

  where s_B is known because it equals the expander inlet entropy, and all other points are on the saturation line and therefore can be found using (13).

- C is a point in the superheated vapor region. This is the case for the expander outlet and the isentropic expander outlet in Figure 3(a), the expander outlet in Figure 3(b), the expander inlet and the isentropic expander inlet in Figure 3(c). The isobaric lines are not straight in this section, but they are assumed linear so that (13) can be applied using the saturated vapor line and the reference line, albeit with less accuracy.

3.3.2 Expander and Pump

Some expander and pump state points cannot be directly found via interpolation and are estimated using the methods described in this section.

Expander Inlet and Outlet

The calculations of expander inlet and expander outlet depend on the characteristics of the fluid and on the expander efficiency η_{exp}.

Working fluids can be classified as *dry fluids* and *wet fluids* according to the shape of their saturation lines and this has significant implications on ORC system design and efficiency (Hung 2001; Mago, Chamra, and Somayaji

 10.3384/ECP207127 DOI

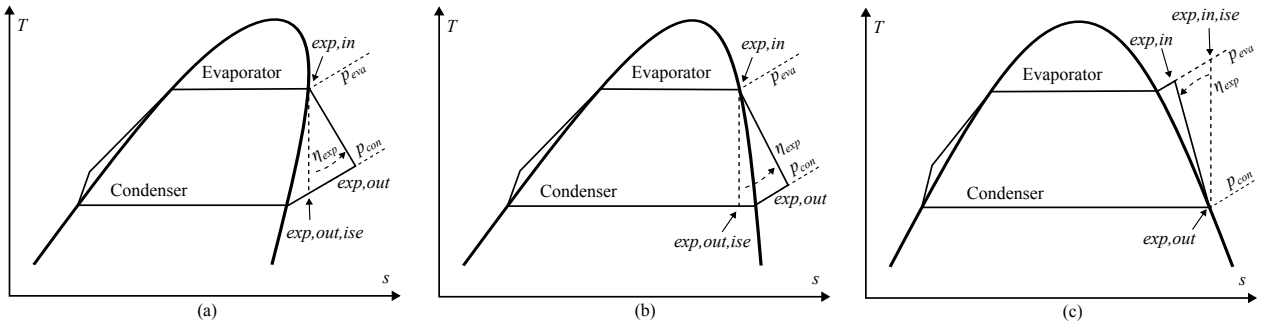

Figure 4. Characteristics of the fluid and the cycle. (a) Dry fluid, dry cycle; (b) wet fluid, dry cycle; (c) wet fluid, wet cycle.

2007; B.-T. Liu, Chien, and C.-C. Wang 2004; Yu, Feng, and Y. Wang 2016). On T-s charts, a dry fluid has a section of positive slope on its saturated vapor line, as shown in 4(a); whereas a wet fluid does not, as shown in 4(b) and (c). Dry fluids are preferable for ORC because as the expansion starts from the saturated vapor line, there is no risk of condensation in the expander. Therefore, superheating before expansion is not needed. For a wet fluid, whether exp, out will be under the dome depends on η_{exp} as well as the location of exp, in.

With the objective to minimise the superheating temperature difference ΔT_{sup} and with η_{exp} known, we distinguish the following two computational paths:

- We call a *dry cycle* a cycle in which the expansion starts from the saturated vapor line (i.e. $\Delta T_{sup} = 0$) and ends in the superheated vapor region. For either a dry fluid or a wet fluid undergoing such a cycle, shown in Figure 4(a) and (b), the expander outlet specific enthalpy $h_{exp,out}$ is obtained from

$$\frac{h_{exp,in} - h_{exp,out}}{h_{exp,in} - h_{exp,out,ise}} = \eta_{exp}. \tag{15}$$

- We call a *wet cycle* a cycle in which the expansion starts from the superheated vapor region and ends on the saturated vapor line. This way ΔT_{sup} assumes the smallest value without causing condensation at expander outlet. In this scenario, the expander inlet specific enthalpy $h_{exp,in}$ is obtained from

$$\frac{h_{exp,in} - h_{exp,out}}{h_{exp,in,ise} - h_{exp,out}} = \eta_{exp}. \tag{16}$$

Pump Outlet

The pump outlet state is obtained from

$$h_{pum,out} = h_{pum,in} + w_{pum}. \tag{17}$$

In our Modelica implementation, the pump power consumption is estimated from fluid work and efficiency as

$$P_{pum} = \frac{\dot{V}\,\Delta p}{\eta_{pum}}. \tag{18}$$

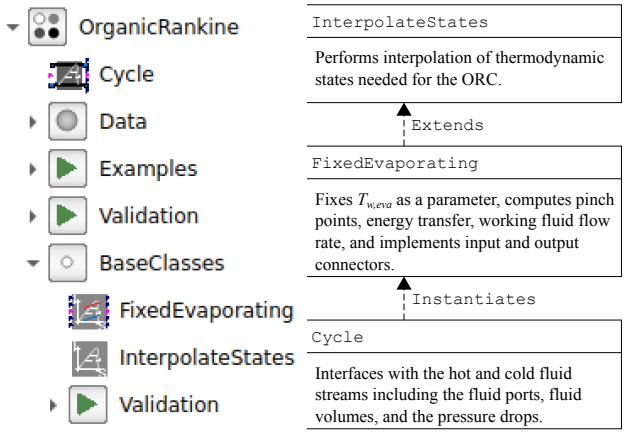

Figure 5. A screenshot from the the package browser and a structure diagram of the implementation

Dividing both sides of (18) by $\dot{m}_w$ yields the specific pump work

$$w_{pum} = \frac{\Delta p}{\rho_w\,\eta_{pum}}. \tag{19}$$

Using the pump inlet state for ρ_w and expanding Δp yields

$$w_{pum} = \frac{p_{eva} - p_{con}}{\rho_{pum,in}\,\eta_{pum}}. \tag{20}$$

This approximation takes advantage of the negligible density change of liquid to avoid property search in the subcooled liquid region and an additional reference line.

In section 5.1, we will validate the above pump work approximation assuming constant density against the pump work estimated from the isentropic process using CoolProp, similar to the expander work in Equation 15, i.e.

$$\frac{h_{pum,out,ise} - h_{pum,in}}{h_{pum,out} - h_{pum,in}} = \eta_{pum}. \tag{21}$$

4 Modelica Package Structure

Inside the Modelica package, the ORC model was implemented in three levels, as shown in Figure 5. At the

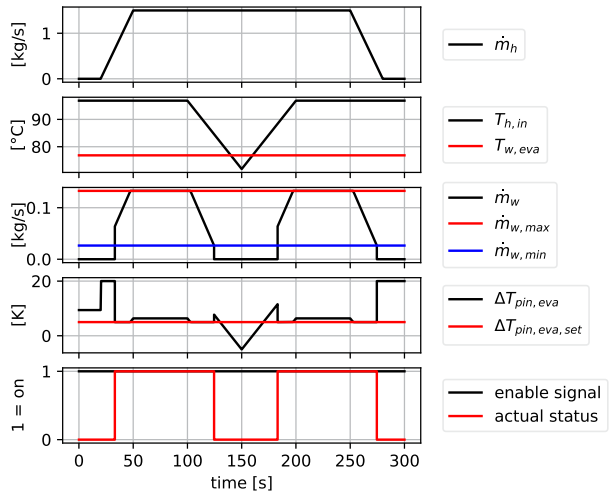

Figure 6. Model validation with variable hot fluid incoming temperature and flow rate

lowest level, thermodynamic property interpolation for the ORC was implemented in `InterpolateStates`. This functionality is in its standalone model for two reasons. First, thermodynamic property estimations from the interpolation schemes are easy to be validated against property tables. Second, this model has no constraints that are imposed by the cycle and its control. When extended by `FixedEvaporating`, various constraints are imposed on the cycle computation to satisfy control objectives described in sections 2 and 3.1. Having the unconstrained model `InterpolateStates` available by itself makes it easy to add different ORC models in the future. At the intermediate level, `FixedEvaporating` adds calculation of $\dot{m}_w$, $T_{pin,eva}$, and $T_{pin,con}$, which are central to the control objectives of the modelled system. At the top level, `Cycle` finally involves the hot and cold fluid streams and is ready to be integrated into an energy system.

5 Model Validation

5.1 Medium Property

The fluid property interpolation implemented in Modelica was validated by comparing its results against direct property readings from CoolProp. Tests were performed with five dry and five wet working fluids to compare results for the specific energy terms

$$w_{exp} = h_{exp,out} - h_{exp,in}, \tag{22}$$

$$w_{pum} = h_{pum,out} - h_{pum,in}, \tag{23}$$

$$q_{eva} = h_{exp,in} - h_{pum,out}, \tag{24}$$

and

$$q_{con} = h_{pum,in} - h_{exp,out}, \tag{25}$$

using the error term

$$err_y = \frac{y_M - y_C}{y_C}, \tag{26}$$

Fluid			ORC Setup			Results		Errors			
	M [g/mol]	T_{cri} [°C]	T_{eva} [°C]	T_{con} [°C]	ΔT_{sup} [K]	η_{the} (Modelica)	η_{the} (CoolProp)	(w_{exp})	(w_{pum})	(q_{eva})	(q_{con})	(η_{the})
Dry												
n-Heptane	100	267	147	37	0	20.1%	19.2%	3.6%	1.3%	-0.5%	-1.5%	4.2%
n-Pentane (R601)	72	197	112	37	0	16.8%	16.6%	0.2%	0.9%	-0.5%	-0.6%	0.7%
Toluene	92	319	173	37	0	23.3%	24.7%	-6.1%	1.4%	-0.6%	1.2%	-5.7%
R123	153	184	105	37	0	16.3%	16.4%	-1.4%	0.9%	-0.5%	-0.3%	-1.1%
R245fa	134	154	91	37	0	13.4%	13.6%	-1.3%	0.8%	-0.3%	-0.2%	-1.1%
Wet												
Acetone	58	235	131	37	5.9	23.1%	23.1%	0.3%	1.2%	0.1%	0.0%	0.2%
Ethanol	46	242	134	37	41.1	26.1%	26.5%	-2.2%	1.6%	-0.6%	0.0%	-1.7%
Propane (R290)	44	97	62	37	3.9	7.4%	7.3%	1.6%	0.5%	0.1%	0.0%	1.7%
R134a	102	101	64	37	4.2	8.2%	8.0%	1.5%	0.4%	0.1%	0.0%	1.5%
R32	52	78	53	37	14.3	4.8%	4.6%	3.7%	0.3%	0.2%	0.0%	4.2%

Table 2. Working fluids properties, experiment setup, results, and errors.

where the subscript M represents Modelica and C represents CoolProp. All tests use $T_{eva} = T_{cri} - 20\,\text{K}$, $T_{con} = 310\,\text{K}$, $\eta_{exp} = 0.8$ and $\eta_{pum} = 0.7$. Their properties, experiment setup, and errors are listed in Table 2.

Table 2 shows the largest errors in w_{exp}. This is thought to be caused by the linear approximation in the superheated region, namely for $h_{exp,in}$ in the case of wet cycles and for $h_{exp,out}$ in the case of dry cycles, and affecting η_{the}. The maximum error is for w_{exp} and η_{the} for Toluene, with

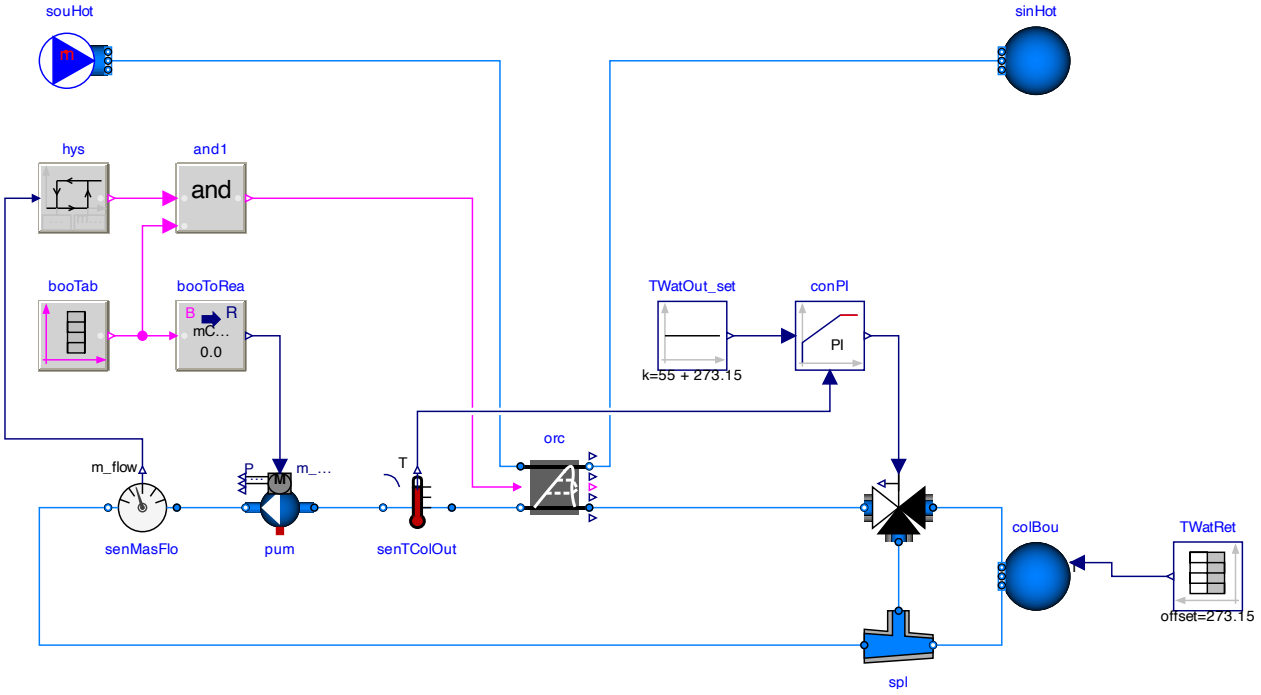

Figure 7. Modelica graphics of the example model where the ORC component is integrated in a district heating system.

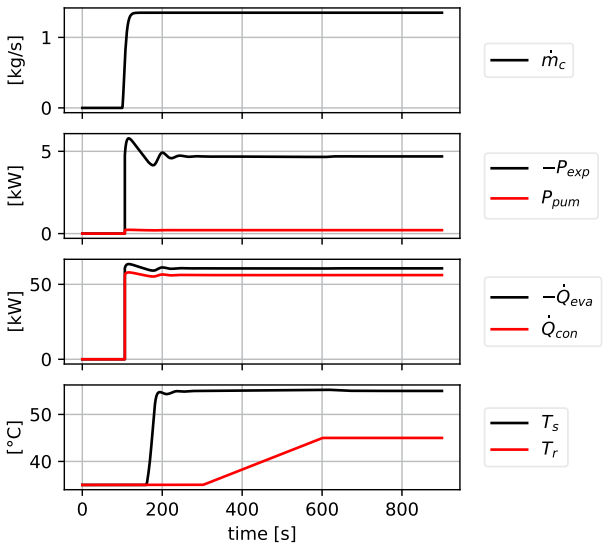

Figure 8. Results output of the example model.

an error of 6.1% and 5.7%, respective. All other errors are below 5%.

Our property computation results agree with the thermodynamic analysis performed by Borsukiewicz-Gozdur (2013), H. Liu, Shao, and Li (2011), and Chen et al. (2006).

5.2 Pinch Point

We conducted a validation to test the constraints on $\dot{m}_w$. We used R245fa as working fluid with $T_{w,eva} = 350$ K, $\Delta T_{pin,eva} = 5$ K, $\Delta T_{pin,con} = 10$ K.

Figure 6 shows how the model deals with a waste heat source whose temperature and flow rate are both variable. It goes through the following stages:

- At $t = 0$, $T_{h,in}$ is sufficiently high but $\dot{m}_h$ is too low. The cycle does does not start ($\dot{m}_w = 0$ and "actual status" is `off`). The set point for $\Delta T_{pin,eva}$ is ignored.
- As $\dot{m}_h$ goes higher, the cycle starts ($\dot{m}_w > 0$ and "actual status" is `on`) when $\dot{m}_h > \dot{m}_{w,min} + \Delta m_{hys}$, where Δm_{hys} is a parameter for the mass flow rate hysteresis. At this stage, $T_{pin,eva}$ is maintained at its set point.
- With $\dot{m}_h$ increasing further, $\dot{m}_w$ reaches its upper limit and no longer increases along with $\dot{m}_h$. $\Delta T_{pin,eva}$ is allowed to go higher than its set point.
- Then at $t = 100$, $T_{h,in}$ starts to decrease. $\dot{m}_w$ is again able to maintain $\Delta T_{pin,eva}$ at its set point shortly after, before the cycle shuts down again when $T_{h,in}$ becomes too low.
- From $t = 150$ the stages above run again in reverse order.

6 Example Model

We integrated our ORC model in a hypothetical district energy system as an example. The model graphics is shown in Figure 7. The hot water return from the system is connected through the ORC condenser, acting as the ORC cold fluid. The mixing valve is modulated with

a PI loop controlling the cold fluid outgoing temperature (i.e. district hot water supply temperature).

The working fluid is R123. It is a dry fluid, i.e. no superheating in the cycle.

Carrying waste heat, the evaporator hot fluid is air, with a constant flow rate and a constant incoming temperature.

The condenser cold fluid represents water from a district heating system. A dedicated condenser pump is used to maintain a constant water flow rate through the condenser. The district hot water return temperature T_r (i.e. the condenser cold fluid incoming temperature $T_{c,in}$ of the ORC) fluctuates between 35 to 45°C. The ORC is controlled to lift its temperature to a supply temperature T_s of 55°C. Additionally, a safety control is implemented to prevent the cycle from starting until the water flow in the condenser is established, i.e. $\dot{m}_c > \dot{m}_{c,threshold}$.

Nominal conditions of this model are shown in Table 3. Simulation results of key variables of this example model are shown in Figure 8.

Quantity	Value	Unit	Quantity	Value	Unit
T_{eva}	100	°C	$\dot{m}_h$	1	kg/s
T_{con}	59.5	°C	$T_{h,in}$	150	°C
p_{eva}	786	kPa	$T_{h,out}$	90.2	°C
p_{con}	282	kPa	$\dot{m}_c$	1.4	kg/s
η_{exp}	0.8	-	$T_{c,in}$	45	°C
η_{pum}	0.6	-	$T_{c,out}$	55	°C
$\dot{m}_w$	0.34	kg/s	η_{the}	7.7%	-

Table 3. Example model nominal conditions.

7 Discussion

We envision that that the model can be further developed in the future to address the following.

Table 2 shows that the interpolation schemes are highly accurate in energy transfer calculation with errors up to 1.6% for w_{pum}, q_{eva}, and q_{con}. For w_{exp} and η_{the}, the highest error was 6.1% and 5.7% with toluene. These higher errors appear to be caused by the linear approximation of isobars in the superheated vapor region and related to the specific characteristics of the fluids. Deeper understanding in this will be valuable in deciding how the medium simplification can be modified to achieve higher accuracy. Note that the validation was intentionally designed to have a very high evaporating temperature ($T_{eva} = T_{cri} - 20$ K) to test extreme cases. Real-world subcritical applications may not use such a high T_{eva} and the model estimation would be more accurate.

Although machine analysis is beyond the scope of this study and we leave the expander efficiency to the user to specify, it is nonetheless important to note that the computation of expander efficiency is important and can improve the estimation accuracy of the model.

In our current model, we used a simple ORC architecture without considering subcooling, recuperating, multiple-stage expansion, or throttling. Supporting more sophisticated architectures such as reviewed by (Lecompte et al. 2015) can expand the general utility of this model.

8 Conclusion

In this work we reported a Modelica implementation of an ORC model. Our model fills the gap of a general-use, open-source ORC model in Modelica with both the following features: a working fluid model that is ready to use or easy to add, and the ability to be integrated into a larger energy system. Because the working fluid selection is an important design decision in ORC system design, our method opens up the ability to choose working fluids from a pool of candidates for an early-stage analysis of ORC system integration. This relieves modellers from the challenges of developing a large number of detailed and computationally efficient medium models. This also results in a standalone model that does not depend on external software for fluid property queries, improving usability and compatibility.

Acknowledgements

This research was supported by the Assistant Secretary for Efficiency and Renewable Energy, Office of Building Technologies and Industrial Efficiency and Decarbonization Office of the U.S. Department of Energy, under Contract No. DE-AC02-05CH11231.

Data Availability

This is an open-source development. At the time of writing, the data and code used in this study are available at Modelica Buildings Library (Wetter et al. 2014) through commit `4d9b7fd` and will be released in future versions of the Modelica Buildings Library.

Nomenclature

Quantities:

c_p	specific heat capacity at constant pressure
h	specific enthalpy
M	molar mass
$\dot{m}$	mass flow rate
P	power
p	pressure
$\dot{Q}$	heat flow rate
q	specific heat flow
s	specific entropy
T	temperature
$\dot{V}$	volumetric flow rate
w	specific work
x	vapor quality
η	efficiency
ρ	density

Subscripts:

c	cold fluid

ele	electrical
h	hot fluid
hys	hysteresis
in	incoming, inlet
ise	isentropic
out	outgoing, outlet
pin	pinch point
w	working fluid
con	condenser
cri	critical
eva	evaporator
exp	expander
pum	pump
sup	superheating
the	thermal

References

Abadi, Gholamreza Bamorovat and Kyung Chun Kim (2017). "Investigation of organic Rankine cycles with zeotropic mixtures as a working fluid: Advantages and issues". In: *Renewable and Sustainable Energy Reviews* 73, pp. 1000–1013.

Asimptote (2023). *FluidProp*. https://asimptote.com/fluidprop/. Date accessed: 22-Oct-2023.

Bao, Junjiang and Li Zhao (2013). "A review of working fluid and expander selections for organic Rankine cycle". In: *Renewable and sustainable energy reviews* 24, pp. 325–342.

Bell, Ian H. et al. (2014). "Pure and Pseudo-pure Fluid Thermophysical Property Evaluation and the Open-Source Thermophysical Property Library CoolProp". In: *Industrial & Engineering Chemistry Research* 53.6, pp. 2498–2508. DOI: 10.1021/ie4033999. eprint: http://pubs.acs.org/doi/pdf/10.1021/ie4033999. URL: http://pubs.acs.org/doi/abs/10.1021/ie4033999.

Borsukiewicz-Gozdur, Aleksandra (2013). "Pumping work in the organic Rankine cycle". In: *Applied Thermal Engineering* 51.1-2, pp. 781–786.

Casella, Francesco and Alberto Leva (2005). "Object-oriented modelling & simulation of power plants with modelica". In: *Proceedings of the 44th IEEE Conference on Decision and Control*. IEEE, pp. 7597–7602.

Chen, Yang et al. (2006). "A comparative study of the carbon dioxide transcritical power cycle compared with an organic Rankine cycle with R123 as working fluid in waste heat recovery". In: *Applied thermal engineering* 26.17-18, pp. 2142–2147.

Hung, Tzu-Chen (2001). "Waste heat recovery of organic Rankine cycle using dry fluids". In: *Energy Conversion and management* 42.5, pp. 539–553.

Imran, Muhammad et al. (2020). "Dynamic modeling and control strategies of organic Rankine cycle systems: Methods and challenges". In: *Applied Energy* 276, p. 115537.

Lecompte, Steven et al. (2015). "Review of organic Rankine cycle (ORC) architectures for waste heat recovery". In: *Renewable and sustainable energy reviews* 47, pp. 448–461.

Liu, Hao, Yingjuan Shao, and Jinxing Li (2011). "A biomass-fired micro-scale CHP system with organic Rankine cycle (ORC)–Thermodynamic modelling studies". In: *Biomass and Bioenergy* 35.9, pp. 3985–3994.

Liu, Bo-Tau, Kuo-Hsiang Chien, and Chi-Chuan Wang (2004). "Effect of working fluids on organic Rankine cycle for waste heat recovery". In: *Energy* 29.8, pp. 1207–1217.

Mago, Pedro J, Louay M Chamra, and Chandra Somayaji (2007). "Performance analysis of different working fluids for use in organic Rankine cycles". In: *Proceedings of the Institution of Mechanical Engineers, Part A: Journal of Power and Energy* 221.3, pp. 255–263.

Manente, Giovanni et al. (2013). "An Organic Rankine Cycle off-design model for the search of the optimal control strategy". In: *Energy* 58, pp. 97–106.

Modelica 3rd-party libraries (2023). *ExternalMedia*. https://github.com/modelica-3rdparty/ExternalMedia. Date accessed: 23-Oct-2023.

Nami, Hossein et al. (2018). "Gas turbine exhaust gas heat recovery by organic Rankine cycles (ORC) for offshore combined heat and power applications-Energy and exergy analysis". In: *Energy* 165, pp. 1060–1071.

Oliveira, Miguel Castro, Muriel Iten, and Henrique A Matos (2022). "Simulation and assessment of an integrated thermal processes and Organic Rankine Cycle (ORC) system with Modelica". In: *Energy Reports* 8, pp. 764–770.

Pan, Lisheng and Weixiu Shi (2016). "Investigation on the pinch point position in heat exchangers". In: *Journal of Thermal Science* 25, pp. 258–265.

Quoilin, Sylvain, Richard Aumann, et al. (2011). "Dynamic modeling and optimal control strategy of waste heat recovery Organic Rankine Cycles". In: *Applied energy* 88.6, pp. 2183–2190.

Quoilin, Sylvain, Adriano Desideri, et al. (2014). "ThermoCycle: A Modelica library for the simulation of thermodynamic systems". In: *10th international Modelica conference*.

Quoilin, Sylvain, Martijn Van Den Broek, et al. (2013). "Techno-economic survey of Organic Rankine Cycle (ORC) systems". In: *Renewable and sustainable energy reviews* 22, pp. 168–186.

Saleh, Bahaa et al. (2007). "Working fluids for low-temperature organic Rankine cycles". In: *Energy* 32.7, pp. 1210–1221.

Twomey, Braden Lee (2016). "Dynamic simulation and experimental validation of an Organic Rankine Cycle model". In.

U.S. DOE (2021-04). *Waste Heat to Power*. https://betterbuildingssolutioncenter.energy.gov/sites/default/files/attachments/Waste_Heat_to_Power_Fact_Sheet.pdf. Date accessed: 15-Aug-2023.

U.S. DOE (2024). *Decarbonizing the U.S. Economy by 2050: A National Blueprint for the Buildings Sector*. URL: https://www.energy.gov/eere/articles/decarbonizing-us-economy-2050.

Wetter, Michael et al. (2014). "Modelica Buildings Library". In: *Journal of Building Performance Simulation* 7.4, pp. 253–270.

Yu, Haoshui, Xiao Feng, and Yufei Wang (2016). "Working fluid selection for organic Rankine cycle (ORC) considering the characteristics of waste heat sources". In: *Industrial & Engineering Chemistry Research* 55.5, pp. 1309–1321.

Zimmer, Dirk (2020). "Robust object-oriented formulation of directed thermofluid stream networks". In: *Mathematical and Computer Modelling of Dynamical Systems* 26.3, pp. 204–233. DOI: 10.1080/13873954.2020.1757726. URL: https://doi.org/10.1080/13873954.2020.1757726.

Zimmer, Dirk, Michael Meißner, and Niels Weber (2022). "The DLR ThermoFluid Stream Library". In: *Electronics* 11.22. ISSN: 2079-9292. DOI: 10.3390/electronics11223790. URL: https://www.mdpi.com/2079-9292/11/22/3790.